Site-Directed Mutagenesis of Dendrotoxin K Reveals Amino Acids Critical for Its Interaction with Neuronal K^+ Channels†

Leonard A. Smith,*,‡ Paul F. Reid,‡ Fan C. Wang,§ David N. Parcej,§ James J. Schmidt,‡ Mark A. Olson,‡ and J. Oliver Dolly§

Department of Immunology and Molecular Biology, Toxinology Division, United States Army Medical Research Institute of Infectious Diseases, Fort Detrick, Frederick, Maryland 21702-5011, and Department of Biochemistry, Imperial College, London SW7 2AY, U.K.

Received December 18, 1996; Revised Manuscript Received April 9, 1997⊗

ABSTRACT: Dendrotoxin K (DTX_K) is a 57-residue protein from mamba venom that blocks certain non-inactivating, voltage-activated K^+ currents in neurones. In order to pinpoint the residues responsible for its specificity, structure−activity relations of DTX_K were investigated by mutagenesis. A previously cloned gene encoding this toxin [Smith *et al*. (1993) *Biochemistry 32*, 5692−5697] was used to make single mutations; after expression in *Escherichia coli* as fusion proteins and enzymatic cleavage of the conjugates isolated from the periplasmic space, nine toxins were purified. Structural analysis of the native DTX_K and representative mutants by circular dichroism showed that no significant differences were detectable in their folded structures. The biological activity of the mutants, which contained alterations of positively charged and other amino acids, was determined from their abilities to compete for the binding of ^{125}I-labeled DTX_K to K^+ channels in synaptic plasma membranes from rat cerebral cortex. Mutants with residues substituted in the α-helix near the C-terminus (R52A or R53A) yielded binding parameters similar to those of wild-type and native DTX_K. In the case of the β-turn (residues 24−28), however, altering single amino acids reduced binding to the high-affinity site of K^+ channels, with the rank order of decreases being K26A ≫ W25A > K24A = K28A. Also, substitutions made in the 3_{10}-helix (residues 3−7), a region located close to the β-turn, produced equivalent effects (K3A > K6A). Thus, it is deduced that residues in the distorted β-turn and neighboring 3_{10}-helix of DTX_k are critical for its interaction with neuronal K^+ channels.

Dendrotoxins isolated from the venoms of snakes belonging to the *Dendroaspis* genus are a family of low molecular weight (∼7K) proteins of 57−60 residues, each having three conserved disulfide bonds. Seven neurotoxic dendrotoxins have been purified from mamba venoms thus far, and the complete amino acid sequence of five (*1*−*3*) and the partial sequence of two (*4*) have been determined. These homologous dendrotoxins are among the most potent blockers of voltage-sensitive K^+ channels discovered (*5*, *6*) to date, acting in the nanomolar range (*7*, *8*). α-Dendrotoxin (α-DTX)[1] purified (*9*) from *Dentroaspis angusticeps* has been utilized for the localization (*5*, *10*) and purification (*11*, *12*) of mammalian brain K^+ channels (*13*). Additionally, some α-DTX homologues display striking selectivity for certain K^+-channel subtypes. In particular, dendrotoxin K (DTX_K) from the venom of *Dentroaspis polylepis* and its close relative δ-DTX from *D. angusticeps* venom have been shown to inhibit preferentially a non-inactivating voltage-dependent K^+ channel in rat ganglionic neurons, while a slow-inactivating current is more susceptible to α-DTX (*8*, *14*, *15*). Similarly, acceptors for α-DTX and δ-DTX show distinct, though overlapping distributions in rat central nervous system (*10*, *16*).

The three-dimensional X-ray crystal structure of α-DTX (*17*) and the NMR solution structures of DTX_I from *D. polylepis* (*18*) and DTX_K (*19*) have been solved; their global polypeptide fold is very similar. DTX_K has a 3_{10}-helix composed of residues 3−7, a β-hairpin of residues 18−35, and an α-helix from residue 47 to residue 56. The three toxin structures determined resemble Kunitz-type, serine protease inhibitors, such as bovine pancreatic trypsin inhibitor (BPTI). Due to a conserved pattern of disulfide bridging, the backbone of the dendrotoxins and the serine protease inhibitors is similar, though subtle differences exist in their detailed structures (*17*). Nonetheless, the dendrotoxins do not exhibit anti-protease activity (*2*, *20*, *21*), and the serine protease inhibitors such as BPTI are unable to block voltage-dependent K^+ channels (*22*).

Despite the availability of the tertiary structure of DTX_K, little is known about the residues or domains that underlie its neurotoxicity. To facilitate investigation on structure−activity relations, the gene encoding DTX_K has been cloned and the protein expressed in *Escherichia coli* and purified in a fully active form (*23*). In this paper, genetically modified cDNAs were used to produce site-directed mutants of DTX_K. Analysis of the resultant proteins yielded new insight into the interactions that govern DTX_K binding to

† This work was supported by a grant (to J.O.D.) from the Medical Research Council (U.K.).

* Author to whom correspondence should be addressed (Tel 301-619-4238 and FAX 301-619-2348).

‡ U.S. Army Medical Research Institute of Infectious Diseases.

§ Imperial College.

⊗ Abstract published in *Advance ACS Abstracts,* June 1, 1997.

[1] Abbreviations: DTX, dendrotoxin; NMR, nuclear magnetic resonance; BPTI, bovine pancreatic trypsin inhibitor; MBP, maltose-binding protein; PCR, polymerase chain reaction; cDNA, complementary DNA; IPTG, isopropyl β-D-thiogalactopyranoside; HPLC, high-pressure liquid chromatography; TFA, trifluoroacetic acid; SDS−PAGE, sodium dodecyl sulfate−polyacrylamide gel electrophoresis; CD, circular dichroism.

S0006-2960(96)03105-4 CCC: $14.00

Table 1: Oligonucleotide Primers Used To Produce Site-Directed Mutations in DTX_K

DTX_K mutant	primer
K3A	5′-ATTTACAGTACGctgCAGCGGATCC-3′
K6A	5′-GCGAAGAGGCAAtgcACAGTACTTTGC-3′
K24A	5′-TGCTTTCCAtgcGTAGTAG-3′
W25A	5′-TTTGCTTTtgcTTTGTAGTA-3′
K26A	5′-ATTGTTTTGCtgcCCATTTG-3′
A27K	5′-GCATTGTTTtttTTTCCATTTG-3′
K28A	5′-GGCATTGtgcTGCTTTCC-3′
R52A	5′-ACAGGTGCGggcGCATTCCTCT-3′
R53A	5′-AACACAGGTggcGCGGCATTCC-3′

K^+ channels, and this may aid the design of effective channel modulators.

EXPERIMENTAL PROCEDURES

Materials. Restriction endonucleases and DNA-modifying enzymes were products of New England Biolabs (Beverly, MA) and Life Technologies (Gaithersburg, MD). The Muta-Gene phagemid *in vitro* mutagenesis kit was purchased from Bio-Rad Laboratories (Hercules, CA). The Wizard DNA purification system was obtained from Promega (Madison, WI). A protein fusion and purification system was supplied by New England Biolabs. Oligonucleotides used for mutagenesis (Table 1) and DNA sequencing were synthesized on an Applied Biosystems 381A instrument (Foster City, CA).

Methods. Nucleic acid manipulations, transformations, plasmid purifications, and affinity chromatography were carried out according to manufacturers' specifications.

Construction and Expression of DTX_K and Its Mutants. Cloning of a cDNA encoding DTX_K and its expression as a maltose-binding protein (MBP) fusion protein in *E. coli* have been described (*23*). DTX_K cDNA was reconstructed by using PCR techniques to eliminate the naturally occurring leader sequence. PCR primers were designed from cDNA sequence data to incorporate unique restriction enzyme sites flanking the structural gene region of DTX_K. The 3′ PCR primer provided a unique *Hin*dIII site, while the 5′ primer duplicated the entire multiple cloning site, as well as the factor X_a protease recognition sequence represented in the cloning vector pMAL-p2. The reconstructed gene was cleaved with restriction endonucleases *Sac*I and *Hin*dIII, gel purified, and ligated to similarly prepared vector DNA. The recombinant plasmid was cloned into *E. coli* DH5α cells.

The wild-type DTX_K gene described above was used as a template for site-directed mutagenesis. The gene cassette, encoding the factor X_a protease recognition site and DTX_K, was removed from the pMAL-p2 vector with restriction endonucleases *Bam*HI (5′ site) and *Hin*dIII (3′ site) and directionally cloned into mutagenesis phagemid vectors pTZ18U and/or pTZ19U. The recombinant plasmids were introduced into *E. coli dut, ung* strain CJ236 (*24*, *25*). After superinfection of recombinant *E. coli* CJ236 cells with the helper phage, M13K07, single-stranded uracil-containing DNA was extracted and purified from phagemid particles.

Mutagenic oligonucleotides (Table 1) were annealed to the single strand template. The complementary strand DNA was synthesized by using T4 DNA polymerase and joined by using T4 DNA ligase. The resulting double-stranded DNA was transformed into *E. coli* strain MV1190, which provided a strong selection against the nonmutagenized strand of the double-stranded DNA based on its uracil content (*24*, *25*). The parental, uracil-containing strand was inactivated, and the strand containing the mutation was replicated. *E. coli* DH5α cells were transformed with the double-stranded DNA containing the mutation(s). DNA, isolated from minipreparations, was analyzed by using the dideoxynucleotide chain termination method with [α-^{35}S]dATPαS and *Taq* DNA polymerase. DTX_K genes containing the correct mutations were excised from the pTZ phagemid vector with *Bam*HI and *Hin*dIII restriction enzymes, directionally subcloned back into a pMALp2 expression vector, and introduced into *E. coli* DH5α cells. Transformants from *E. coli* DH5α cells were grown at 37 °C in Terrific broth (*26*) containing 100 μg/mL ampicillin to a cell density of $(2-4) \times 10^8$ cells/mL. Protein induction was then initiated by adding isopropyl β-D-thiogalactopyranoside (IPTG) to the culture (final concentration, 0.6 mM), and the cells were harvested 2.5 h later.

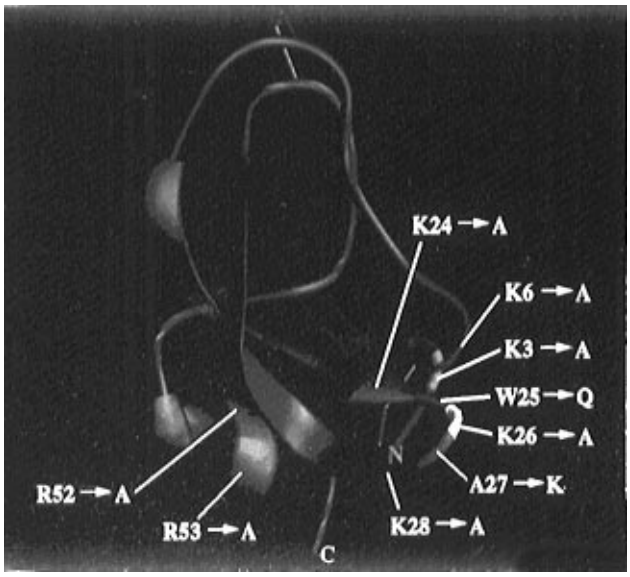

FIGURE 1: Three-dimensional representation of the averaged-minimized NMR structure of DTX_K illustrating the various constructed mutants. Regions of the molecule colored blue are unchanged, and the remaining colored regions denote each substitution. Disulfide bridges are colored yellow.

Purification and Characterization of Recombinant DTX_K and DTX_K Mutants. Cells containing the pMALp constructs were lysed by osmotic shock (*27*) in 5 mM $MgSO_4$ containing 10 μM pepstatin A and 10 μM leupeptin. After centrifugation, periplasmic extracts containing MBP-DTX_K were applied to an amylose affinity resin as previously described (*23*) and unbound proteins removed by washing the amylose resin with buffer A (10 mM sodium phosphate, pH 7.2, 30 mM NaCl, and 1 mM sodium azide) containing 0.25% (v/v) Tween 20. The bound MBP-DTX_K fusion protein was eluted by buffer A containing 15 mM maltose. Fusion proteins were cleaved at 26 °C for 24−48 h by using factor X_a in buffer B (20 mM Tris-HCl and 100 mM NaCl, pH 8.0) at a ratio of 0.1−0.5% (w/w) of factor X_a (1000 units/mg) to the fusion protein. Products of the factor X_a cleavage were applied to an Alltech Vydac 218 TP column (250 mm × 4.6 mm, 5 μm) (Deerfield, IL) equilibrated with 0.1% (v/v) TFA in water. Proteins were eluted from the column by using a linear gradient of acetonitrile in the latter. Fractions containing the recombinant DTX_K or DTX_K mutants were lyophilized, resuspended

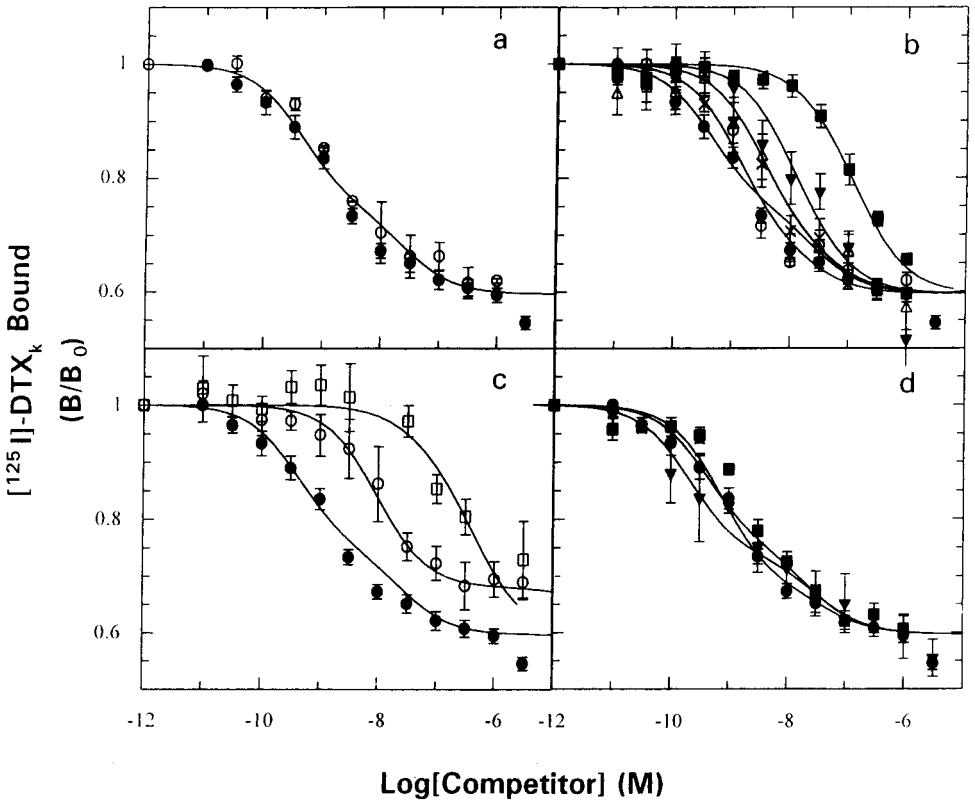

FIGURE 2: Effects of site-directed mutagenesis of DTX_K on binding to neuronal K^+ channels. Rat synaptic plasma membranes from cerebral cortex were incubated at room temperature for 1 h in the presence of 1 nM ^{125}I-DTX_K and various concentrations of native or recombinant DTX_K or its mutants, and binding was measured as described. Values (± SD, $n = 13$ for native DTX_K; $n = 3-5$ for recombinant DTX_K and its mutants) are plotted for the fractional binding in the absence (B_0) and presence (B) of (a) native (●) and wild-type recombinant DTX_K (○); (b) mutants K24A (×), W25A (▼), K26A (■), A27K (○), and K28A (△) from the β-turn; (c) mutants K3A (□) and K6A (○) of the 3_{10}-helix; and (d) mutants R52A (■) and R53A (▼) in the α-helix region.

in 20 mM sodium phosphate, pH 7.4 (buffer C), and applied to an HPLC cation-exchange column (Waters SP-8HR) equilibrated in buffer C. The samples were eluted by a linear gradient of NaCl (0−1 M) prepared in buffer C. Toxin-containing fractions were desalted using a Sep Pak C-18 column, lyophilized, and resuspended in water. Recombinants were analyzed by SDS−PAGE under reducing conditions in Novex (San Diego, CA) precast gradient Tricine gels (10−20%). Purified recombinant DTX_K and selected DTX_K mutants were subjected to N-terminal sequencing by automated Edman degradation performed by a model 470A amino acid sequencer from Applied Biosystems (Foster City, CA).

Purification and Iodination of Native Dendrotoxins. DTX_K and α-DTX were purified from the venoms of *D. polylepis* and *D. angusticeps*, respectively, as previously described (*9*). DTX_K was radioiodinated by a modification of the chloramine-T method to a specific activity of 300−800 Ci/mmol, as detailed before (*9*, *28*).

Circular Dichroic (CD) Measurements. CD spectra were recorded on a JASCO spectropolarimeter J720 in the far-UV (185−255 nm) and near-UV (245−325 nm) range, using 0.2 and 1 cm path lengths, respectively. A time constant of 4 s, a scan rate of 10 nm/min, and a bandwidth of 2 nm were used. The spectra are expressed as $\Delta\epsilon = \epsilon_L - \epsilon_R$ (M^{-1} cm^{-1}) based on a mean molecular weight per amino acid residue, in accordance with pending IUPAC-IUB recommendations.

Molecular Modeling Methods. Atomic coordinates used for modeling DTX_K consisted of 20 NMR determined conformers, taken from the Brookhaven Protein Data Bank (accession number 1DTK). An averaged structure was computed and energy minimized with the consistent valence force field partial charge set of Discover (Biosym Technologies Inc., San Diego, CA). Electrostatic surface potential maps were calculated for the averaged-minimized structure and several NMR structures, by using the program GRASP (*29*). The physiological ionic strength was set at 0.145 M, and dielectric constants of 80 and 4 were used for the solvent and protein interior, respectively. Molecular modeling of protein ribbon diagrams was constructed by using the program RIBBONS (*30*).

Purification of Synaptic Plasma Membranes. These were isolated from rat cortex, as previously described (*28*), and resuspended by homogenization in 7 mM imidazole hydrochloride buffer (pH 7.4) containing 2 mM EDTA, 25 μg/mL bacitracin, 10 μg/mL soybean trypsin inhibitor, 0.2 mM benzamidine, and 0.1 mM phenylmethanesulfonyl fluoride. Membranes were stored at −70 °C.

Binding Assay. Inhibition of the binding of ^{125}I-DTX_K to rat synaptic membranes by unlabeled toxin or mutants was carried out in 50 mM imidazole hydrochloride, 90 mM NaCl, 5 mM KCl, and 1 mM $SrCl_2$, pH 7.4, as previously described (*23*). Membranes were incubated at room temperature for 1 h in the presence of 1 nM ^{125}I-DTX_K and various concentrations of unlabeled toxin (native, recombinant wild-type, or mutated DTX_K). Bound toxin was separated from free toxin by centrifuging through a mixture of silicone fluid and dinonyl phthalate. The pellets were counted in a

Table 2: K_i Values for the Inhibition of ^{125}I-DTX_K Binding by DTX_K and Its Mutants

competitor DTX_K	K_{i1} (nM) site 1	K_{i2} (nM) site 2	B_{max} (pmol/mg) site 1	B_{max} (pmol/mg) site 2	P^a
native	0.26 ± 0.15	48 ± 51	0.29 ± 0.07	2.9 ± 2.6	<0.002
Rec WT-DTX_K	0.29 ± 0.12	135 ± 189	0.29 ± 0.01	2.9 ± 0.5	<0.0001
mutated in					
β-turn					
K24A	0.94 ± 0.51				
W25A	2.8 ± 0.7				
K26A	51 ± 9				
A27K	0.14 ± 0.03				
K28A	0.84 ± 0.24				
3_{10}-helix					
K3A	324 ± 87				
K6A	3.9 ± 1.3				
α-helix					
R52A	0.18 ± 0.09				
R53A	0.57 ± 0.21				

[a] Goodness of fit of the data to a two-site versus a single-site model was determined by the *F*-test (*28*), compared to a *P* value of 0.05 recommended by the latter.

γ-counter. Data were analyzed by using the LIGAND program (*31*).

RESULTS

Site-Directed Mutagenesis and Characterization of Purified Mutants of DTX_K. Specific mutations (Figure 1) in the DTX_K gene were initially shown to be correct by nucleotide sequence analysis (data not shown). Purity of the recombinant DTX_K and its mutants was established from analysis by SDS−PAGE and reverse-phase chromatography followed by cation-exchange chromatography. Furthermore, the first 15 residues of wild type and mutants K3A and K6A, as well as 30 residues for mutant K26A, were shown by automated Edman degradation to have the correct amino acid sequences.

Identification of Residues in DTX_K Important for Binding to Neuronal K^+ Channels. The DTX_K mutants were tested for their ability to compete for binding of 1 nM ^{125}I-DTX_K to K^+ channels. Rat synaptic plasma membranes were chosen for assaying the mutants because of an adequate level of specific binding for DTX_K and the unavailability of a cell line expressing sufficient quantities of recombinant K^+ channels. Native and recombinant wild-type DTX_K each exhibited extended competition curves for inhibition of ^{125}I-DTX_K binding (Figure 2a), which allowed two apparent sites (termed 1 and 2) to be resolved using the LIGAND program. The B_{max} values derived for the two sites using native DTX_K are 0.29 (R_1) and 2.9 (R_2) pmol/mg of protein; identical figures were obtained when wild-type toxin was employed. The analysis yielded equilibrium binding constants of 0.26 (K_{i1}), 48 (K_{i2}) nM for native and 0.29 (K_{i1}), 135 (K_{i2}) nM for wild-type recombinant DTX_K, respectively (Table 2). The appropriateness of the two-site model compared to the one-site version for native and wild-type recombinant DTX_K was shown using an *F*-test (*31*), which revealed a significant improvement [$P < 0.002$ and $P < 0.0001$, respectively, well below the threshhold of 0.05 recommended (*31*)], when the data are fitted to the two-site model. The close agreement of the two sets of K_i values for native and wild-type recombinant DTX_K is indicative of the expressed protein being fully active and, thus, correctly folded (see below). High uncertainty was observed for the low-affinity site probably due to the relatively low concentration of labeled ligand that had to be used to ensure a tolerable level of nonsaturable binding and/or the high degree of interdependence of the above-noted parameters (R_1, R_2, K_{i1}, and K_{i2}) on the two-site model (*31*). Therefore, only the high-affinity binding site is dealt with further in this paper.

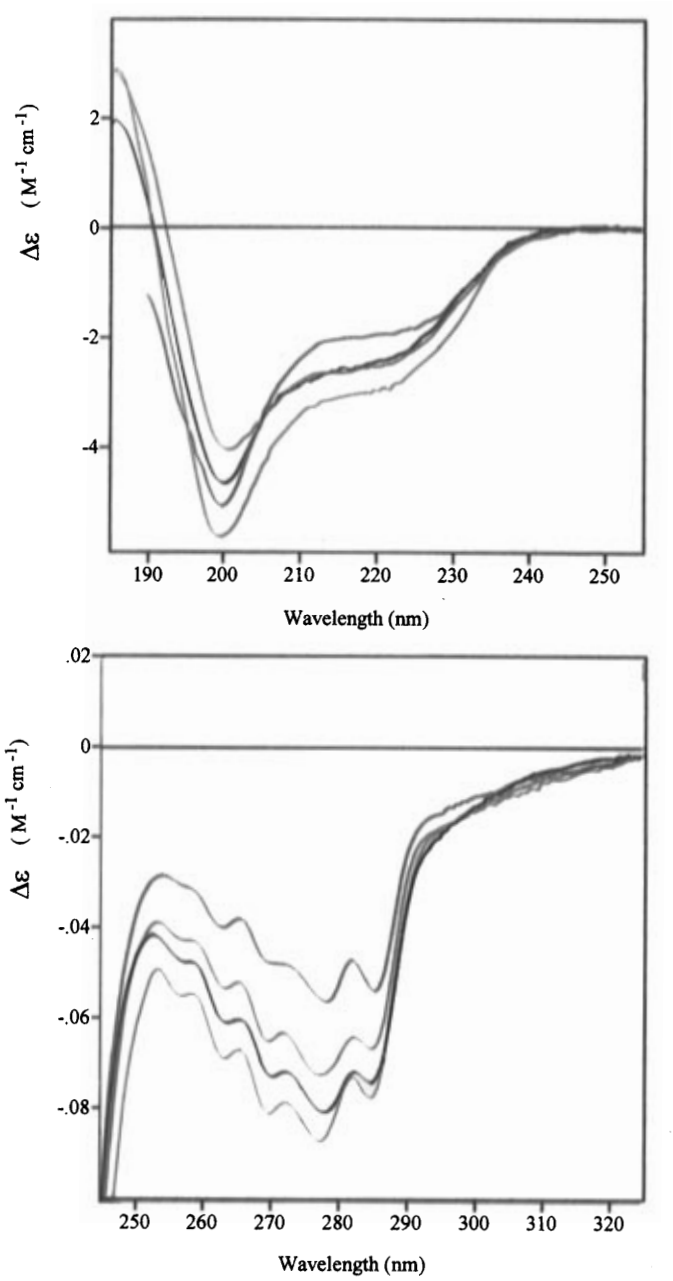

FIGURE 3: Ultraviolet circular dichroic (CD) spectra of DTX_K and mutants. The CD spectra of native DTX_K (blue) and mutants K3A (green), K6A (red), and K26A (black) were recorded in the far- (a, top panel, 185−255 nm) and near- (b, bottom panel, 245−325 nm) UV range, with a JASCO spectropolarimeter J720 using a 4 s time constant, a 10 nm/min scan speed, and a spectral bandwidth of 2 nm. Similarity in the far-UV spectra for native and the recombinant toxins suggests that the mutations did not cause misfolding of the backbone. The profiles observed for the mutants at 290 nm and above are almost identical to that for native toxin, indicating that formation of S−S bridges and the local structure of W25 (the only one present in the toxin) are unaltered. A noted increase or decrease of the negative ellipticity between 250 and 290 nm may be due to changes in local freedom of Y and F residues.

Mutational analysis concentrated principally on positively charged residues in three well-defined regions of DTX_K that

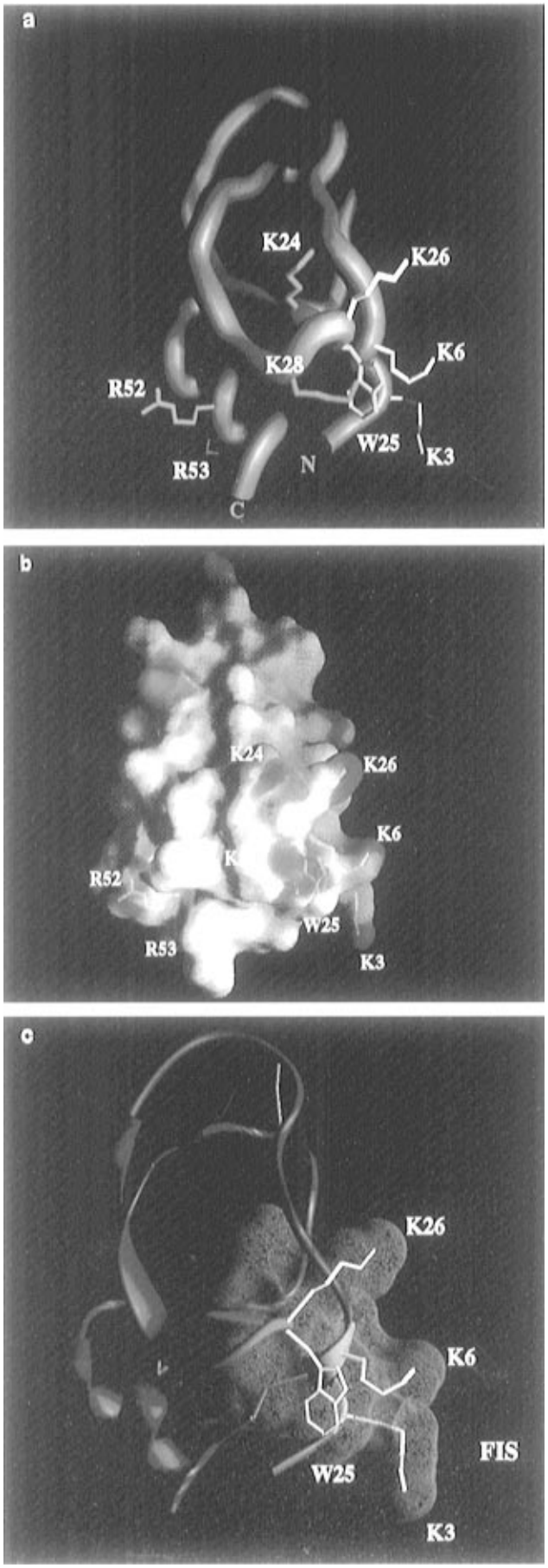

FIGURE 4: Models showing the folded structures and charge density distribution of DTX_K and the residues found to be essential for its interaction with K^+ channels. (a) Main-chain folding of DTX_K showing the side-chain positions of mutated residues: K3 and K6 of the 3_{10}-helix; K24, W25, K26, and K28 of the β-turn; and R52 and R53 of the α-helical region. (b) Electrostatic surface map of the conformer presented in (a) with blue and red representing positive and negative charges, respectively. Note the cluster of positive charges in the region shown by mutagenesis to contain amino acids (c, see below) that are required for the high-affinity binding of DTX_K to neuronal K^+ channels. (c) A cross section of the solvent-accessible surface is shown (in rose color) for the above-mentioned residues, and the side chains of the key residues are depicted in white. The three disulfide bonds are indicated in yellow.

are distinguishable in its NMR structure (*19*). Five of the mutants studied form part (residues 24−28) of the distorted β-hairpin. Substituting positively charged residues (K24, K26, or K28) in the β-turn with alanine resulted in decreased binding affinity for site 1 (Figure 2b), with the K26A mutant giving the most dramatic decrease ($K_{i1} = 51$ nM) compared to a value of 0.29 nM for wild-type DTX_K (Table 2). Introduction of a lysine instead of alanine at position 27 increased slightly the affinity for site 1. Additionally, mutation of tryptophan at position 25 to a less hydrophobic residue (alanine) yielded a 10-fold reduction in affinity for site 1 (Table 2). Thus, both positively charged and a hydrophobic residue in this domain are involved in the high-affinity interaction of DTX_K with K^+ channels.

Although separated in the primary sequence from the β-turn by about 20 amino acids, changing K6 or K3 to alanine in the 3_{10}-helix yielded large reductions (13−1113-fold) in the binding affinity for site 1, which may give rise to the incomplete inhibition observed (Figure 2c). Moreover, inspection of the DTX_K structure obtained by NMR revealed that these residues are in close proximity to the β-turn. Thus, the data reveal that these positively charged residues as well as those adjacent to the β-hairpin (K26 and to a lesser extent K24 and K28) along with W25 located in the latter region are functionally important for the high-affinity binding of DTX_K to synaptic membranes.

Unlike alteration of amino acids in the above-mentioned two regions, mutation of two positively charged residues (R52A, R53A) in the α-helix at the C-terminus had little influence on the binding of DTX_K to K^+ channels (Figure 2d). Such a lack of effect highlights the selectivity of the other changes that lowered the affinity for K^+ channels.

Assessment of the Structural Effects of Representative Mutations. It is conceivable that the dramatic reduction of binding affinity caused by the aforementioned changes might be due to a gross structural alteration in the toxin molecule. This possibility was examined by recording both the near- and the far-UV circular dichroic (CD) spectra (Figure 3) for native DTX_K and three mutants (K3A, K6A, and K26A). These proteins showed similar spectra in the far-UV range (Figure 3a), illustrating that the backbones are similarly folded. This was corroborated by the negative ellipticity above 290 nm (Figure 3b), due to the three S−S chromophores (*32*), which is virtually identical for each of the proteins, suggesting that the disulfide bonds are formed correctly. Even the local structure around the tryptophan at position 25 seems not to have been affected by the mutations; this was shown (Figure 3b) by the similar profile around 290 nm (*32*). Likewise, the good concordance of the absorption of the tyrosine and phenylalanine residues between 250 and 290 nm in the near-UV spectra for these mutants also indicated that the local environment around

these residues was not altered. Nevertheless, the observed decrease (for K3A and K26A) or increase (for K6A) in the intensity of the negative ellipticity may reflect a change in their freedom. However, such changes in local freedom do not appear to affect the binding of DTX_K to K^+ channels because these three particular mutants all exhibited similarly reduced affinity.

DISCUSSION

The structural framework for selecting and characterizing the various mutants was based on the idea of a positively charged region of DTX_K interacting, in an appropriate topology, with a complementary negatively charged region on the K^+ channel (*21*, *23*, *33*). Such a presumption arose from the multiple lysines and/or arginines that are conserved only in DTX_K and other homologues that block the K^+ channel (*7*, *34*). Accordingly, high salt concentrations lower the affinity of DTX for K^+ channels (*12*), presumably by disturbing such electrostatic interactions, a change also achieved by removal of a glutamate from the toxin binding domain in K^+ channel α subunits (*35*). In addition, complementary mutagenesis of the Kv1.3 channel α subunit and charybdotoxin, kaliotoxin, margatoxin, noxiustoxin, and other peptide K^+ channel blockers revealed multiple toxin-channel points of association including electrostatic interactions (*36*) involving positively charged toxin residues similar to that seen here and acidic amino acids in the channel mouth.

The DTX_K residues mutated are shown in the overall three-dimensional fold of the protein (Figure 4a). The calculated electrostatic potential map (Figure 4b) associated with the molecular surface of the averaged NMR solution structure of DTX_K (*19*) reveals that all of the residues altered, K3 and K6 in the 3_{10}-helix, K24, K26, and K28 of the *β*-turn, and R52 and R53 in the α-helix, are located in highly solvent-exposed areas which are strongly charged (cf. Figure 4a,c). The aggregate charge density appears to be significantly compacted along the base of the molecule (Figure 4b), with the side chains of K26 (mutation of which gave rise to more than a 100-fold reduction in affinity) and K28 of the *β*-turn and K3 and K6 of the 3_{10}-helix protruding out into the solvent (Figure 4c). Importantly, the residues found to be critical for the high-affinity interaction of the toxin with the K^+ channel reside in these two structural elements. With the exception of A27K (see below), all of the mutations examined in the *β*-turn and 3_{10}-helix lowered the binding affinity for site 1 of K^+ channels. Substitution of A by K at position 27, mimicking the *β*-turn of α-DTX, led to a slight increase in binding affinity. Interestingly, however, the inhibition curve for this mutant resembles the one-site pattern of inhibition reported for α-DTX (*28*). Although interaction of DTX_K with synaptosomal membranes appears complex (see Figure 2), probably due to the several K^+ channel subtypes present (*37*), this does not affect any of the conclusions presented. Interestingly, in the case of the homologous protein, α-DTX, mutation of a triple lysine cluster in the *β*-turn decreased binding to neuronal K^+ channels, but the shift was much less dramatic (*38*) than those seen herein. This quantitative difference probably reflects the subtle dissimilarity in the structures of α-DTX (*17*) and DTX_K (*19*) that probably underlies their distinct specificities for different K^+-channel subtypes (*14*, *15*, *39*). From this study, it can be deduced that the *β*-turn and 3_{10}-helix domains are particularly important for interaction with K^+ channels. This information may aid in producing artificial and selective K^+-channel blockers.

ACKNOWLEDGMENT

The authors thank Matthew Hinz and Lancer Cuddy for their technical support. Computational studies were supported by a grant (to M.A.O.) from the Frederick Biomedical Supercomputing Center of the Frederick Cancer Research and Development Center. We thank Dr. Giuliano Siligardi and the National Chiroptical Spectroscopy Facility (EPSRC) service for recording and analyzing CD spectra.

REFERENCES

1. Strydom, D. J. (1973) *Nature 243*, 88−89.
2. Joubert, F. J., and Taljaard, N. (1980) *Hoppe-Seyler's Z. Physiol. Chem. 361*, 661−674.
3. Mehraban, F., Haines, A., and Dolly, J. O. (1986) *Neurochem. Int. 9*, 11−22.
4. Benishin, C. G., Sorensen, R. G., Brown, W. E., Krueger, B. K., and Blaustein, M. P. (1988) *Mol. Pharmacol. 34*, 152−159.
5. Halliwell, J. V., Othman, I. B., Pelchen-Matthews, A., and Dolly, J. O. (1986) *Proc. Natl. Acad. Sci. U.S.A. 83*, 493−497.
6. Stansfeld, C. E., Marsh, S. J., Parcej, D. N., Dolly, J. O., and Brown, D. A. (1987) *Neuroscience 23*, 893−902.
7. Dolly, J. O., Muniz, Z. M., Parcej, D. N., Hall, A. C., Scott, V. E. S., Awan, K. A., and Owen, D. G. (1994) in *Neurotoxins in Neurobiology* (Tipton, K. F., and Dajas, F., Eds.) pp 103−122, Ellis Horwood Ltd., Chichester.
8. Hall, A., Stow, J., Sorensen, R., Dolly, J. O., and Owen, D. (1994) *Br. J. Pharmacol. 113*, 959−967.
9. Dolly, J. O. (1992b) in *Receptor−Ligand Interactions: A Practical Approach* (Hulme, E. C., Ed.) pp 37−61, IRL Press, Oxford.
10. Pelchen-Matthews, A., and Dolly, J. O. (1989) *Neuroscience 29*, 347−361.
11. Rehm, H., and Lazdunski, M. (1988) *Proc. Natl. Acad. Sci. U.S.A. 85*, 4919−4923.
12. Parcej, D. N., and Dolly, J. O. (1989) *Biochem. J. 257*, 899−903.
13. Dolly, J. O., and Parcej, D. N. (1996) *J. Bioenerg. Biomembr. 28*, 231−253.
14. Stuhmer, W., Ruppersberg, J. P., Schroter, K. H., Sakmann, B., Stocker, M., Giese, K. P., Perschke, A., Baumann, A., and Pongs, O. (1989) *EMBO J. 8*, 3235−3244.
15. Robertson, B., Owen, D., Stow, J., Butler, C., and Newland, C. (1996) *FEBS Lett. 383*, 26−30.
16. Awan, K., and Dolly, J. O. (1991) *Neuroscience 40*, 29−39.
17. Skarzynski, T. (1992) *J. Mol. Biol. 224*, 671−683.
18. Foray, M. F., Lancelin, J. M., Hollecker, M., and Marion, D. (1993) *Eur. J. Biochem. 211*, 813−820.
19. Berndt, K. D., Guntert, P., and Wuthrich, K. (1993) *J. Mol. Biol. 234*, 735−750.
20. Strydom, D. J. (1976) *Eur. J. Biochem. 69*, 169−176.
21. Harvey, A. L., Anderson, A. J., Mbugua, P. M., and Karlsson, E. (1984) *J. Toxicol. Toxin Rev. 3*, 91−137.
22. Harvey, A. L., Anderson, A. J., Marshall, D. L., Pemberton, K. E., and Rowan, E. G. (1990) *J. Toxicol. Toxin Rev. 9*, 225−242.
23. Smith, L. A., Lafaye, P. J., LaPenotiere, H. F., Spain, T., and Dolly, J. O. (1993) *Biochemistry 32*, 5692−5697.
24. Kunkel, T. A. (1985) *Proc. Natl. Acad. Sci. U.S.A. 82*, 488−492.
25. Kunkel, T. A., Roberts, J. D., and Zakour, R. A. (1987) *Methods Enzymol. 154*, 367−382.
26. Tartof, K. D., and Hobbs, C. A. (1987) *Bethesda Res. Lab. Focus 9*, 12.
27. Neu, H. C., and Heppel, L. A. (1965) *J. Biol. Chem. 240*, 3685−3692.

28. Black, A. R., Breeze, A. L., Othman, I. B., and Dolly, J. O. (1986) *Biochem. J. 237*, 397−404.
29. Nicholls, A., Sharp, K., and Honig, B. (1991) *Proteins: Struct., Funct., Genet. 11*, 281−296.
30. Carson, M. (1987) *J. Mol. Graphics 5*, 103−106.
31. Munson, P. J., and Rodbard, D. (1980) *Anal. Biochem. 107*, 220−239.
32. Hollecker, M., and Larcher, D. (1989) *Eur. J. Biochem. 179*, 87−94.
33. Smith, L. A., Olson, M. A., Lafaye, P. J., and Dolly, J. O. (1995) *Toxicon 33*, 459−474.
34. Harvey, A. L., and Anderson, A. J. (1985) *Pharmacol. Ther. 31*, 33−55.
35. Hurst, R. S., Busch, A. E., Kavanaugh, M. P., Osbourne, P. B., North, R. A., and Adelman, J. P. (1991) *Mol. Pharmacol. 40*, 572−576.
36. Aiyar, J., Withka, J. M., Rizzi, J. P., Singleton, D. H., Andrews, G. C., Lin, W., Boyd, J., Hanson, D. C., Simon, M., Dethlefs, B., Lee, C. L., Hall, J. E., Gutman, G. A., and Chandy, K. G. (1995) *Neuron 15*, 1169−1181.
37. Scott, V. E. S., Muniz, Z. M., Sewing, S., Lichtinghagen, R., Parcej, D. N., Pongs, O., and Dolly, J. O. (1994) *Biochemistry 33*, 1617−1623.
38. Danse, J. M., Rowan, E. G., Gasparini, S., Ducancel. F., Vatanpour, H., Young, L. C., Poorheidari, G., Lajeunesse, E., Drevet, P., Menez, R., Pinkasfeld, S., Boulain, J.-C., Harvey, A. L., and Menez, A. (1994) *FEBS Lett. 356*, 153−158.
39. Robertson, B., Owen, D. G., Stow, J., Butler, C. A., and Newland, C. F. (1994) *J. Physiol. 481*, 41−42.

BI963105G